

Article

Not peer-reviewed version

Structural, Electronic, and Optical Properties of Anisotropic Rutile Titanium Dioxide: A Density Functional Theory Study

[Desta Regassa Golja](#) * and [Megersa Olumana Dinka](#)

Posted Date: 7 March 2025

doi: 10.20944/preprints202503.0482.v1

Keywords: anisotropic-TiO₂; density functional theory; bandgap; density of states; dielectric function; photocatalytic applications



Preprints.org is a free multidisciplinary platform providing preprint service that is dedicated to making early versions of research outputs permanently available and citable. Preprints posted at Preprints.org appear in Web of Science, Crossref, Google Scholar, Scilit, Europe PMC.

Copyright: This open access article is published under a Creative Commons CC BY 4.0 license, which permit the free download, distribution, and reuse, provided that the author and preprint are cited in any reuse.

Article

Structural, Electronic, and Optical Properties of Anisotropic Rutile Titanium Dioxide: A Density Functional Theory Study

Desta Regassa Golja ^{1,2,*} and Megersa Olumana Dinka ²

¹ Department of Civil Engineering Science, Faculty of Engineering and the Built Environment, Johannesburg, South Africa

² Department of Applied Physics, School of Applied Natural Sciences Adama Science and Technology University, Adama, Ethiopia

* Correspondence: regasdd12@gmail.com

Abstract: This study investigates the structural, electronic, and optical properties of anisotropic rutile titanium dioxide (TiO₂) using density functional theory (DFT). The calculated lattice parameters were found to be $a = b = 4.64 \text{ \AA}$ and $c = 42.97 \text{ \AA}$. The generalized gradient approximation (GGA) exchange-correlation functional predicted a bandgap of 1.89 eV, in close agreement with experimental results. A detailed analysis of the density of states (DOS) and projected density of states (PDOS) further validated the accuracy of the computed bandgap. The optical properties were examined through the dielectric function, revealing real and imaginary static dielectric constants of 11.85 and 0.13, respectively. Moreover, the absorption and conductivity spectra exhibited promising behavior in the UV-visible range, indicating strong potential for water remediation and photocatalytic applications. Overall, the electronic and optical characteristics of TiO₂ suggest its viability as an effective material for environmental and energy-related applications.

Keywords: anisotropic-TiO₂; density functional theory; bandgap; density of states; dielectric function; photocatalytic applications

1. Introduction

Titanium dioxide (TiO₂) has garnered significant attention in various fields due to its remarkable properties, including high stability, non-toxicity, and excellent photocatalytic activity. Its applications range from environmental remediation and solar energy conversion to its use in pigments and coatings [1,2]. Although rutile TiO₂ is particularly noted for its photocatalytic applications, a comprehensive understanding of its electronic and optical properties remains critical for optimizing its performance. Various methods have been employed to investigate these properties, including experimental techniques like UV-Vis spectroscopy and advanced computational approaches such as density functional theory (DFT) [1–4]. However, there exist gaps in the literature regarding the detailed electronic structure and light absorption mechanisms of rutile TiO₂, particularly under varying experimental conditions and doping scenarios [3,4]. Currently, hybrid density functionals and first-principles calculations are increasingly utilized to study the electronic and optical characteristics of rutile TiO₂, providing deeper insights that can enhance its efficacy in photocatalytic applications and other technological advancements. Titanium dioxide (TiO₂) has garnered significant attention in various fields due to its remarkable properties, including high stability, non-toxicity, and excellent photocatalytic activity [4,5]. Its applications range from environmental remediation and solar energy conversion to its use in pigments and coatings [1–6]. Although rutile TiO₂ is particularly noted for its photocatalytic applications, a comprehensive understanding of its electronic and optical properties remains critical for optimizing its performance [5,7]. Various methods have been employed to investigate these properties, including experimental techniques like UV-Vis

spectroscopy and advanced computational approaches such as density functional theory (DFT) [6,8]. However, there exist gaps in the literature regarding the detailed electronic structure and light absorption mechanisms of rutile TiO_2 , particularly under varying experimental conditions and doping scenarios. Currently, hybrid density functionals and first-principles calculations are increasingly utilized to study the electronic and optical characteristics of rutile TiO_2 , providing deeper insights that can enhance its efficacy in photocatalytic applications and other technological advancements [7,8]. Titanium dioxide (TiO_2) has gained considerable attention as a photocatalyst due to its exceptional properties, including high stability, nontoxicity, and excellent photocatalytic activity. Among the various polymorphs of TiO_2 , rutile TiO_2 stands out for various applications, like photocatalytic activities in environmental remediation, solar cells as it features a well-defined crystal structure and favorable electronic properties [7–9]. Its ability to facilitate chemical reactions under light irradiation makes it an ideal candidate for applications in environmental remediation, energy conversion, and solar hydrogen production [1–9].

Titanium dioxide (TiO_2) is a versatile material with a wide range of applications due to its unique properties, including high stability, non-toxicity, and strong photocatalytic activity. It is widely employed in photocatalysis for environmental remediation, effectively breaking down pollutants in water and air under UV light [9]. In dye-sensitized solar cells (DSSCs), TiO_2 serves as a semiconductor that facilitates electron transport, enhancing solar energy conversion efficiency. Additionally, TiO_2 is commonly used as a white pigment in paints, coatings, and plastics due to its excellent opacity and reflective properties [6–10]. It's also a critical ingredient in sunscreens, providing physical UV protection for the skin. Furthermore, TiO_2 finds applications in self-cleaning surfaces, food packaging, photonic devices, hydrogen production through photoelectrochemical cells, and various biomedical applications, solidifying its importance in advancing both technological and environmental solutions [10]. The fundamental mechanism of TiO_2 photocatalysis involves the absorption of light, leading to the generation of electron-hole pairs. When exposed to UV light, electrons from the valence band are excited to the conduction band, leaving behind holes. These charge carriers participate in various redox reactions, enabling the degradation of organic pollutants or facilitating water splitting for hydrogen production [10,11]. However, the intrinsic band gap of rutile TiO_2 , approximately 3.0 eV, limits its activity predominantly to the UV region of the solar spectrum [11–13]. This limitation has driven substantial research efforts aimed at modifying the band gap and enhancing light absorption to improve photocatalytic efficiency [12].

Density Functional Theory (DFT) offers a powerful computational framework for exploring the electronic structure of materials and is an invaluable tool in photocatalytic research [12–14]. By employing DFT, researchers can investigate how changes in crystal structure, doping with various elements, or the introduction of surface defects influence the electronic properties and photocatalytic performance of rutile TiO_2 [15]. Specifically, DFT allows for the calculation of band structures, densities of states, and charge distributions, providing insights into the fundamental processes underpinning photocatalysis [16]. Recent advancements in DFT methodologies have enabled the examination of more complex systems, such as TiO_2 composites and heterostructures, which can further enhance photocatalytic efficiency by creating favorable interfaces for charge separation [17]. Doping rutile TiO_2 with metal or non-metal elements leads to the introduction of mid-gap states, effectively narrowing the band gap and enabling the absorption of a broader range of the solar spectrum, including visible light [16–18]. Additionally, the development of mixed-phase photocatalysts that combine rutile with other TiO_2 phases or distinct semiconductor materials has shown promising improvements in photocatalytic activity [12–18]. Given the pressing need for sustainable energy solutions and effective strategies for environmental remediation, investigating rutile TiO_2 as a photocatalyst through the lens of DFT research represents a vital area of study [4–10]. By optimizing its electronic properties and enhancing light absorption capabilities through various modifications, the applicability of rutile TiO_2 can be significantly expanded, paving the way for innovative applications in solar energy conversion and environmental cleanup [18].

This introduction sets the stage for a detailed discussion of the methodologies and findings related to the DFT study of anisotropic rutile TiO₂ as a photocatalyst, underscoring its potential impact in these critical fields.

2. Computational Methods

The first-principles technique was employed with the Quantum Espresso package, which is grounded in density functional theory (DFT). In this computational methodology, the exchange-correlation functional was represented using projector augmented wave (PAW) basis sets. In line with the generalized gradient approximation (GGA) of the Perdew-Burke-Ernzerhof (PBE) were used for band and density of state calculations. The accuracy of DFT calculations primarily depends on the optimization kinetic energy cutoff, k- mesh sampling, and of lattice constants. Prior to these optimization self-consistent relaxation was performed with a threshold energy tolerance of 1.20×10^{-9} eV. A kinetic energy cutoff of 60 Ry was applied for the functions, which determines the number of plane wave expansions within the muffintin radii of the systems. The first irreducible Brillouin zone (BZ) was sampled using a $7 \times 7 \times 8$ Monkhorst-Pack scheme. Moreover, the density of states was determined using a $20 \times 20 \times 22$ k-point sampling set. For the calculations of optical properties, norm-conserving pseudopotentials were applied. This approach allowed us to effectively characterize the electronic and optical behavior of the TiO₂ system. The electronic structures of the core and valence shells of all constituent elements in the compound under investigation are titanium (Ti): [Ar] 3d²4s², and oxygen (O): 2s² 2p⁴. In the tetragonal crystal structure of titanium dioxide (TiO₂), with the space group P4/nmm (No. 136), the Wyckoff positions represent the specific locations of atoms within the unit cell of the crystal. These positions are determined by the symmetry operations of the space group [20–24]. For the space group P4/nmm, the Wyckoff positions for TiO₂ are Ti atoms occupy the 2c Wyckoff position, which means there are 2 symmetry-equivalent positions per unit cell; Oxygen (O) atoms occupy the 2a and 2b Wyckoff positions, which mean there are 2 symmetry-equivalent positions for each oxygen site per unit cell. This can put simply as Ti is at 2c: (1/4, 1/4, z), O is at 2a: (3/4, 1/4, 0) and O is at 2b: (1/4, 3/4, 0). These positions help in understanding the arrangement of atoms in the crystal structure, which is crucial for determining the material's properties [4–10].

3. Results and Discussion

3.1. Crystal Structure

Titanium dioxide exhibits a tetragonal structure and crystallizes in the space group P4₂/mnm, with Wyckoff positions for Ti (2a) and O (2c). The TiO₂ crystal consists of six atoms within its unit cell. For a single component, the bond lengths for Ti-Ti, Ti-O, and O-O are 4.64 Å, 2.00 Å, and 2.87 Å, respectively. In the tetragonal structure, Ti⁴⁺ ions are typically coordinated by four O²⁻ ions. This coordination can lead to distorted tetrahedral configurations in certain local environments, although predominant octahedral coordination is more frequently seen in the rutile phase. O²⁻ ions generally bond with multiple Ti⁴⁺ atoms, resulting in a network of Ti-O bonds that enhances the stability of the crystal structure. The lattice parameters were derived from the optimized TiO₂ crystal structure, resulting in values of a = b = 4.64 and c = 2.97 Å, which align with both theoretical and experimental findings [3–15].

3.2. Band Gaps and Density of States

The electronic band structures of TiO₂ are presented in Figure 2. The band structure is calculated along the high symmetry point in the irreducible Brillouin zone of Γ -X-M- Γ -Z-R-A-Z-X-R-M-A. As illustrated in Figure 2, the conduction band minimum and valence band maximum occur at the same symmetry points, resulting in a direct energy band gap of 1.862 eV, which is consistent with previous studies [21–24]. The Projected densities of states (PDOS) calculations were performed to investigate the unique contributions of various orbitals to the total density of states (TDOS). The

valence band (VB) is mainly shaped by the O-2p orbitals, whereas the conduction band (CB) is primarily composed of Ti-3d states, which confirms the occurrence of TiO₂ d-p hybridization. Furthermore, the small contributions from Ti-p and O-s orbitals indicate that hybridization effects at higher energy levels are minimal.

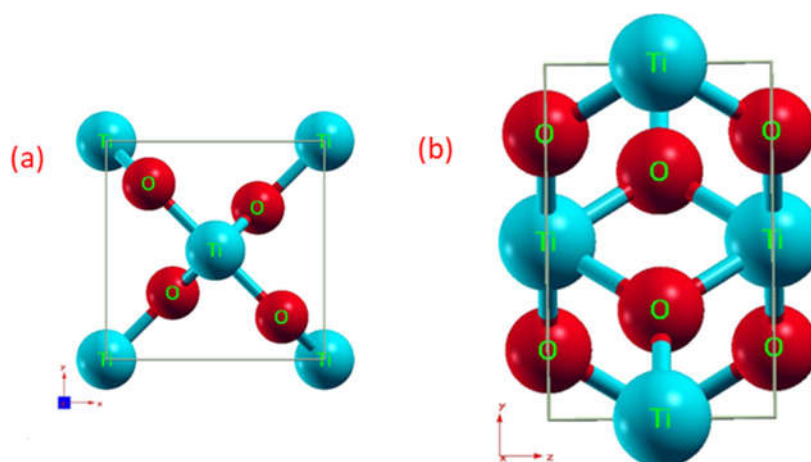


Figure 1. (a) Top and side (b) view of TiO₂ crystal structure.

3.3. Optical Characteristics

The optical characteristics of materials are essential to study from the perspective of industrial manufacturing of optical devices such as sensors, lasers, modulators, solar calculators, optical coating and waste water remediation [10,24]. Figure 2 shows the dielectric functions and loss factor of TiO₂ were analyzed along the three polarization directions, revealing critical insights into the material's optical properties [15–20]. The optical characteristics of the frequency dependence complex dielectric functions are determined using the formula; $\epsilon(\omega) = \epsilon_1(\omega) + i\epsilon_2(\omega)$ where $\epsilon_1(\omega)$ and $\epsilon_2(\omega)$ are real and imaginary dielectric functions. The real dielectric function indicates a material's capability to store electrical energy when subjected to an applied electric field, serving as a crucial indicator of its optical properties.

The highest peaks in the dielectric function were observed at specific energy values, which suggest areas of maximum light absorption and polarization capability of TiO₂ crystal. The analysis of the imaginary dielectric function reveals important insights into the optical properties of the material studied [17,20]. Along the z-plane, a prominent peak was observed at approximately. Energy (E)-3.64 eV, indicating an enhanced absorption, while similar peaks were identified along the x and y plane at slightly different energy levels of 3.61 eV and 3.37 eV, respectively. In the considered energy range, several peaks emerged, with the last energy values of 7.69eV, 8.7eV, and 7.66eV situated within the ultraviolet (UV) region of the electromagnetic spectrum. These values correspond to wavelengths of approximately 161.2 nm, 142 nm, and 162.3 nm, indicating their placement within the deep UV light spectrum. Such high-energy photons are associated with significant electronic transitions in Anisotropic TiO₂. The presence of these peaks suggests that Anisotropic TiO₂ crystal demonstrates strong absorbance in the UV range, which is essential for applications in photocatalysts, UV protection, and various optoelectronic devices [20–24]. This capability for effective UV light absorption highlights the importance of energy conversion and environmental remediation technologies [16,20]. The static dielectric constants of TiO₂ were calculated for all polarizations, resulting in values of 7.31, 7.68, and 9.12, respectively.

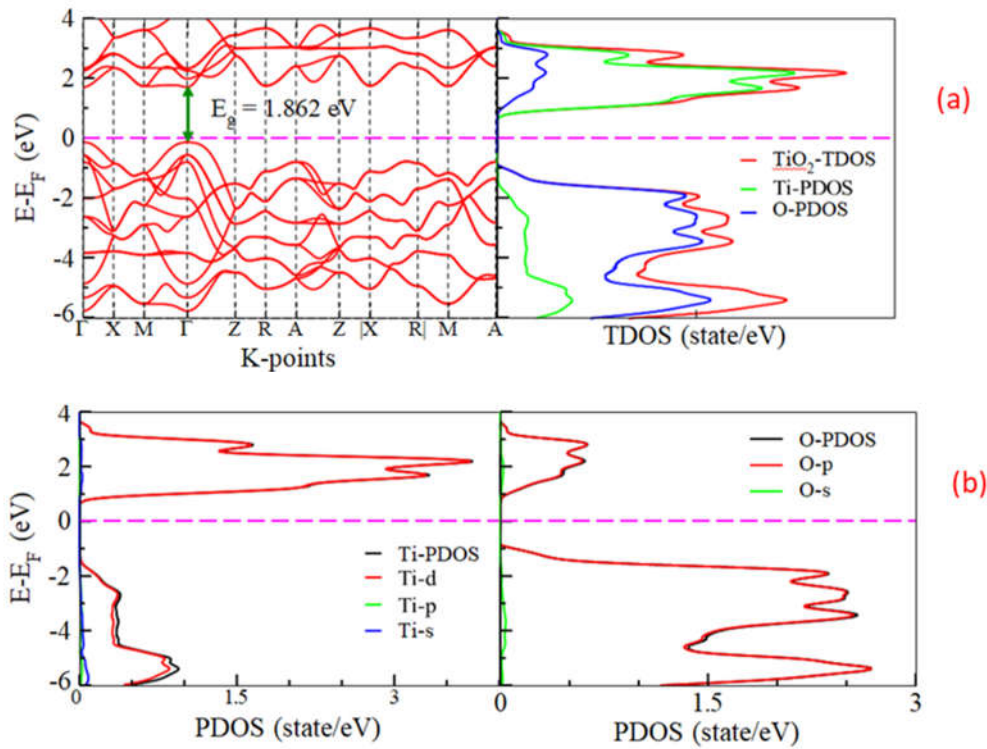


Figure 2. Electronic band structure (a) TDOS of TiO₂ (b) PDOS of Ti and PDOS of oxygen of the tetragonal TiO₂ crystal structure.

The energy loss function is an essential parameter in materials science and technology, particularly for understanding how energy is dissipated as electrons move rapidly through a material (Figure 3(b), (d) and (e)). In particular, as seen in the figures the loss factors, peak values range from 12.5 to 20eV in three planes, indicating an improvement in energy dissipation capacity at these energy levels [5–15]. Overall, understanding these interconnections between the dielectric function and the loss factor, particularly through their peak values, underscores the optical behavior of the material and its potential effectiveness in applications such as photocatalysis and other optoelectronic devices [15,20]. Such analyses can guide further optimization processes in material design for enhanced performance. An in-depth understanding of the optical properties of anisotropic TiO₂, including the refractive index, extinction coefficient, absorption coefficient, and reflectivity, was calculated and plotted in Figure 3 (a-d). The refractive index, extinction coefficient, absorption, and reflectivity of the materials are calculated through one to four equations.

$$n(\omega) = \left\{ \frac{\sqrt{\epsilon_1(\omega)^2 + \epsilon_2(\omega)^2} + \epsilon_1(\omega)}{2} \right\}^{\frac{1}{2}} \text{----- (1)}$$

$$k(\omega) = \left\{ \frac{n!}{r!(n-r)!} \left\{ \frac{\sqrt{\epsilon_1(\omega)^2 + \epsilon_2(\omega)^2} - \epsilon_1(\omega)}{2} \right\}^{\frac{1}{2}} \right\}^{\frac{1}{2}} \text{----- (2)}$$

$$\alpha(\omega) = \frac{4\pi k}{\lambda}$$

$$R = \frac{(1-n)^2 + k^2}{(1+n)^2 + k^2}$$

$$L(\omega) = \frac{\epsilon_2(\omega)}{\epsilon_1(\omega)^2 + \epsilon_2(\omega)^2}$$

Figure 2 (a) represent the refractive index of isotropic TiO₂ along x, y, and z plane exhibits significant peaks at approximately 3.67, 3.00, and 3.41 eV, respectively. Additionally, two peaks are observed at higher energy levels, with prominent peaks around 8.12, 8.10, and 7.48 eV. Beyond these peaks, the refractive index decreases with increasing energy, suggesting a reduced interaction with higher energy photons. The refractive index values appear to increase with energy, suggesting that TiO₂ behaves anisotropically, where the optical response varies depending on the direction of light propagation. Figure 4 (b) shows the extinction coefficient, indicated by the data labeled as k_{xx} , k_{yy} , and k_{zz} , which describes how much light is absorbed or scattered as it passes through the material [4,5,10]. The values provide insight into the loss of intensity of the transmitted light as a result of absorption. Higher extinction coefficients at specific energy levels suggest significant absorption in these regions, which is particularly relevant for TiO₂ in applications where UV absorption is desired. For TiO₂, these peaks in extinction could correlate with electronic transitions that occur when TiO₂ absorbs photons in those regions of the spectrum. The absorption coefficient quantifies how effectively TiO₂ absorbs light as it propagates through the material. Figure 4(c) highlights distinct absorption peaks around 5 eV and 10 eV, indicating strong UV absorption linked to the band gap and electronic transitions.

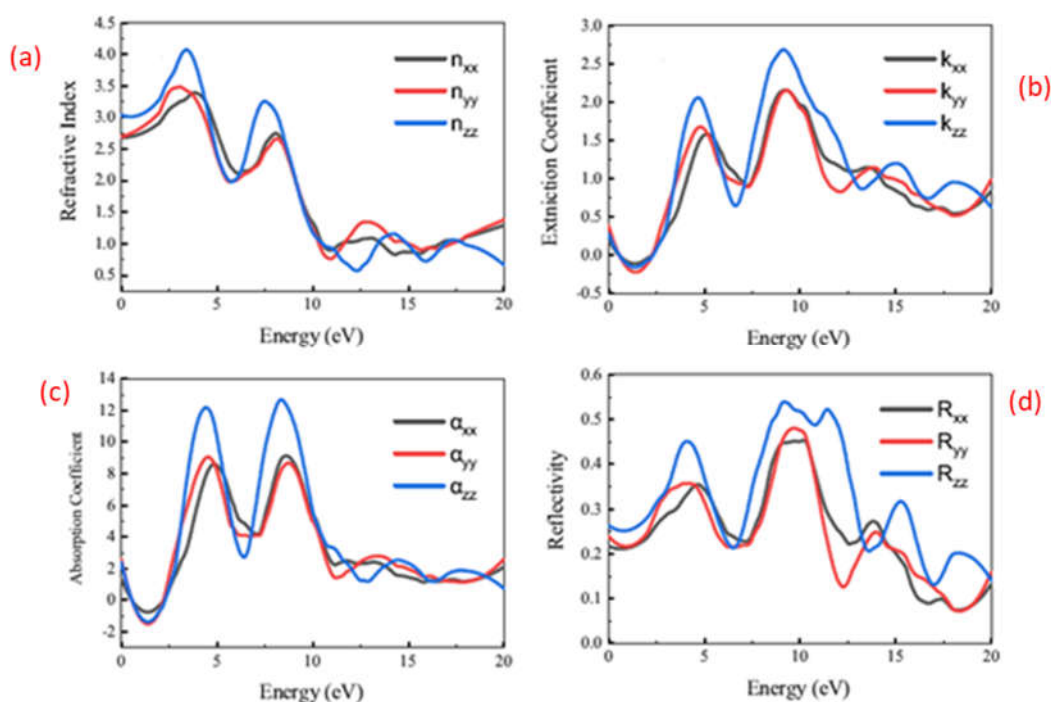


Figure 4. (a) Refractive index, (b) extinction coefficient, (c) absorption coefficient, and (d) Reflectivity of the tetragonal TiO₂ crystal structure.

The highest absorption occurs along the z-axis, reinforcing TiO₂'s anisotropic optical properties. This aligns with prior studies, confirming its suitability for photocatalysis and UV shielding applications. Figure 4(d) illustrates the reflectivity of TiO₂ along different polarization directions. Reflectivity represents the fraction of incident light that is reflected from the material's surface [17,24]. High reflectivity indicates low light absorption, making TiO₂ suitable for applications requiring reflective coatings. Conversely, low reflectivity at specific energy levels suggests efficient absorption, which is beneficial for photocatalytic and solar energy applications. In the low-energy range (0-5eV), TiO₂ exhibits moderate reflectivity, which increases at higher energies, with multiple peaks in the UV and visible regions. The highest reflectivity is observed along the z-axis, emphasizing the material's anisotropic optical behavior. This trend is consistent with previous studies showing that TiO₂ thin films exhibit reflectivity variations based on crystallographic orientation [16,20,24].

4. Conclusions

In conclusion, the structural, electronic and optical properties of the tetragonal crystal structure anisotropic TiO₂ have been investigated using first-principles DFT calculations. The analysis of the refractive index, extinction coefficient, absorption coefficient, and reflectivity of TiO₂ reveals critical information about its optical properties and behavior. The anisotropic nature of TiO₂, as indicated by the different values along different axes, suggests tailored applications depending on the structure and design of the optical devices. The ability of TiO₂ to absorb light effectively in specific energy ranges highlights its suitability for use in photovoltaic applications and photocatalysts. Understanding these optical properties provides valuable insights for optimizing TiO₂ in various technological advancements. Further numerical values and specific graphical data would enhance the depth of this analysis, facilitating more precise conclusions regarding TiO₂ optical performance.

Reference

1. M.A. Gatou, A. Syrrakou, N. Lagopati, E. A. Pavlatou, Photocatalytic TiO₂-based nanostructures as a promising material for diverse environmental applications: a review, *Reactions* 5 (2024) 135–194.
2. N. H. S. Suhaimi, R. Azhar, N. S. Adzis, M. A. M. Ishak, M. Z. Ramli, M. Y. Hamzah, K. Ismail, W. I. Nawawi, Recent updates on TiO₂-based materials for various photocatalytic applications in environmental remediation and energy production, *Desalination and Water Treatment* (2024) 100976.
3. K. Fukuda, I. Fujii, R. Kitoh, I. Awai, Molecular dynamics study of the TiO₂ (rutile) and TiO₂-ZrO₂ systems, *Acta Crystallographica Section B: Structural Science* 49 (1993) 781–783.
4. A. Thilagam, D. Simpson, A. Gerson, A first-principles study of the dielectric properties of TiO polymorphs, *Journal of Physics: Condensed Matter* 23 (2010) 025901.
5. Thilagam, A., Simpson, D.J. and Gerson, A.R., 2010. A first-principles study of the dielectric properties of TiO₂ polymorphs. *Journal of Physics: Condensed Matter*, 23(2), p.025901.
6. Fukuda, K., Fujii, I., Kitoh, R. and Awai, I., 1993. Molecular dynamics study of the TiO₂ (rutile) and TiO₂-ZrO₂ systems. *Structural Science*, 49 (4), pp.781-783.
7. Gatou, M.A., Syrrakou, A., Lagopati, N. and Pavlatou, E.A., 2024. Photocatalytic TiO₂-based nanostructures as a promising material for diverse environmental applications: a review. *Reactions*, 5(1), pp.135-194.
8. Suhaimi, N.H.S., Azhar, R., Adzis, N.S., Ishak, M.A.M., Ramli, M.Z., Hamzah, M.Y., Ismail, K. and Nawawi, W.I., 2025. Recent updates on TiO₂-based materials for various photocatalytic applications in environmental remediation and energy production. *Desalination and Water Treatment*, 321, p.100976.
9. Dong, J. and Drabold, D.A., 1998. Atomistic structure of band-tail states in amorphous silicon. *Physical review letters*, 80(9), p.1928.
10. Valencia S, Marn J M, Restrepo G. Study of the bandgap of synthesized titanium dioxide nanoparticles using the sol-gel method and a hydrothermal treatment. *Open Mater. Sci.* 2010; 4: 9.
11. Cai B, Drabold D A. Properties of amorphous GaN from first-principles simulations. *Phy. Rev. B* 2011; 84: 075216.

12. Robertson, J., 2008. Physics of amorphous conducting oxides. *Journal of non-crystalline solids*, 354(19-25), pp.2791-2795.
13. Manzini I, Antanioli G, Bersani D, Lottici P P, Gnappi G, and Montonero A, X-ray absorption spectroscopy study of crystallization processes in sol-gel-derived TiO₂. *J. Non-Cryst. Solids* 1995; 519:192
14. Shao G. Electronic structures of manganese-doped rutile TiO₂ from first principles. *J. Phys. Chem. C* 2008; 112:18677.
15. Lee, C., Ghosez, P. and Gonze, X., 1994. Lattice dynamics and dielectric properties of incipient ferroelectric TiO₂ rutile. *Physical Review B*, 50(18), p.13379.
16. Lide, D.R. ed., 2004. *CRC handbook of chemistry and physics* (Vol. 85). CRC press.
17. Perdew, J.P., Burke, K. and Ernzerhof, M., 1996. Generalized gradient approximation made simple. *Physical review letters*, 77(18), p.3865.
18. Giannozzi, P., Baroni, S., Bonini, N., Calandra, M., Car, R., Cavazzoni, C., Ceresoli, D., Chiarotti, G.L., Cococcioni, M., Dabo, I. and Dal Corso, A., 2009. QUANTUM ESPRESSO: a modular and open-source software project for quantum simulations of materials. *Journal of physics: Condensed matter*, 21(39), p.395502.
19. Matsui, M. and Akaogi, M., 1991. Molecular dynamics simulation of the structural and physical properties of the four polymorphs of TiO₂. *Molecular Simulation*, 6(4-6), pp.239-244.
20. Nowotny J. Titanium dioxide-based semiconductors for solar-driven environmentally friendly applications: impact of point defects on performance; *Energy Environ. Sci.* 2008; 2:565.
21. Ollis D F, Al-Ekabi H. *Photocatalytic purification and treatment of water and air*. Elsevier: Amsterdam, The Netherlands 1993.
22. Gratzel M. Mesoporous oxide junctions and nanostructured solar cells. *Curr.Opin. Colloid Interface Sci.* 1999; 4:314.
23. Wang Y Q, Chen S G, Tang X H, Palchik O, Zaban A, Kolytyn Y, Gedanken A. mesoporous titanium dioxide: sono-chemical synthesis and application in dye-sensitized solar cells. *J. Mater. Chem.* 2001; 11:521.
24. Rahman M, MacElroy D, Dowling D P. Influence of the physical, structural and chemical properties on the photoresponse property of magnetron sputtered TiO₂ for the application of water splitting. *Journal of Nanoscience and Nanotechnology*, 2011; 11, 8642.

Disclaimer/Publisher's Note: The statements, opinions and data contained in all publications are solely those of the individual author(s) and contributor(s) and not of MDPI and/or the editor(s). MDPI and/or the editor(s) disclaim responsibility for any injury to people or property resulting from any ideas, methods, instructions or products referred to in the content.